

Effects of Temperature, Oxidation and Fiber Preforms on Fatigue Life of Carbon Fiber-Reinforced Ceramic-Matrix Composites

Li Longbiao¹

Received: 19 March 2016 / Accepted: 31 March 2016 / Published online: 14 April 2016
© Springer Science+Business Media Dordrecht 2016

Abstract In this paper, the effects of temperature, oxidation and fiber preforms on the fatigue life of carbon fiber-reinforced silicon carbide ceramic-matrix composites (C/SiC CMCs) have been investigated. An effective coefficient of the fiber volume fraction along the loading direction (ECFL) was introduced to describe the fiber architecture of preforms. Under cyclic fatigue loading, the fibers broken fraction was determined by combining the interface wear model and fibers statistical failure model at room temperature, and interface/fibers oxidation model, interface wear model and fibers statistical failure model at elevated temperatures in the oxidative environments. When the broken fibers fraction approaches to the critical value, the composites fatigue fracture. The fatigue life S–N curves and fatigue limits of unidirectional, cross-ply, 2D, 2.5D and 3D C/SiC composites at room temperature, 800 °C in air, 1100, 1300 and 1500 °C in vacuum conditions have been predicted.

Keywords Ceramic-matrix composites (CMCs) · Fatigue · S-N curve · Life prediction

1 Introduction

With the demand for high thrust-weight ratio and more efficient aero engine, the temperature of the turbine sections will be raised to a level exceeding the limit of current metallic materials. New materials will have to be tested and validated at very high temperatures that surpass 1300 °C. Ceramic-matrix composites (CMCs) are lighter than superalloys and maintaining the structural integrity even at higher temperatures, desirable qualities for improving aero engine efficiency, and have already been implemented on some aero engines' components, i.e., the CMC flaps for exhaust nozzles of SNECMA M53 and M88 aero engines [1, 2]. The CMC

✉ Li Longbiao
llb451@nuaa.edu.cn

¹ College of Civil Aviation, Nanjing University of Aeronautics and Astronautics, No.29, Yudao St., Nanjing 210016, People's Republic of China

turbine vanes have been designed and tested in the aero engine environment under the implementation of Ultra Efficient Engine Technology (UEET) program [3]. A CMC turbine blade has been tested for 4 h by General Electric in a modified GE F414 engine, which represents the first application of the CMC material in a rotating engine component. Incorporating the CMC turbine blades on a GE90–sized engine, the overall weight can be reduced by 455 kg, which represents approximately 6 % of dry weight of a full sized GE90–115 [4]. In these applications, the CMCs will be subjected to varying temperatures, pressures, and degrading environments like water vapor. Such environment can cause rapid oxidation which is a primary mechanism of environmental degradation of CMCs.

Upon first loading to fatigue peak stress, matrix multicracking, fiber/matrix interface debonding, and partially fibers fractured in the interface debonded and bonded region, would occur [5]. With increasing cycle number, interface shear stress decreases due to interface wear when fibers slide relative to matrix during unloading and subsequent reloading, which reduces the load transfer capacity between fibers and the matrix [6]. The fibers strength also degrades with increasing cycle number due to interface wear, which reduces the load carrying capacity of fibers [7]. At elevated temperatures, matrix cracks would serve as avenues for the ingress of environment atmosphere into the composite. When the oxidizing gas ingresses into the composite, a sequence of events is triggered starting first with the oxidation of the interphase, and then fibers. With increasing oxidation time, the oxidation region propagates; and the interface shear stress and fibers strength decrease. Under cyclic fatigue loading, fibers gradually fracture due to the degradation of interface shear stress and fibers strength. When the broken fibers fraction approaches to the critical value, the composites fatigue fail [8, 9].

The objective of this paper is to investigate the effects of temperature, oxidation and fiber preforms on the fatigue life of C/SiC composites. An effective coefficient of the fiber volume fraction along the loading direction (ECFL) was introduced to describe the fiber architecture of the preforms. Under cyclic fatigue loading, the fibers broken fraction was determined by combining the interface wear model and fibers statistical failure model at room temperature, and interface/fibers oxidation model, interface wear model and fibers statistical failure model at elevated temperatures, based on the assumption that the fibers strength is subjected to two-parameter Weibull distribution and the load carried by broken and intact fibers satisfy the Global Load Sharing (GLS) criterion. The fatigue life S–N curves and fatigue limits of unidirectional, cross-ply, 2D, 2.5D and 3D C/SiC composites at room and elevated temperatures have been predicted.

2 Life Prediction Model

Under cyclic fatigue loading, the loading directions were along with the fiber for unidirectional CMCs, 0° fiber ply for cross-ply and plain-weave 2D CMCs, warp yarn for 2.5D CMCs, and axial fibers at a small angle θ for 3D CMCs. An effective coefficient of the fiber volume content along the loading direction (ECFL) is defined as,

$$\psi = \frac{V_{f_axial}}{V_f} \quad (1)$$

where V_f and V_{f_axial} denote the total fiber volume fraction in the composites and the effective fiber volume fraction in the cyclic loading direction. The values of parameter

ψ , which can be used to characterize fiber architectures, corresponding to unidirectional, cross-ply, 2D, 2.5D and 3D C/SiC composites are 1.0, 0.5, 0.5, 0.75 and 0.93. Under cyclic fatigue loading at room and elevated temperatures, the broken fibers fraction in the 0° plies or longitudinal yarns of cross-ply, 2D, 2.5D and 3D CMCs would increase with increasing applied cycles and oxidation time. When the broken fibers fraction in the 0° plies or longitudinal yarns approaches to the critical value, the composites fatigue fracture.

When fibers begin to break, the load dropped by broken fibers would be transferred to intact fibers in the cross-section. The two-parameter Weibull model is adopted to describe the fibers strength distribution. The fibers fracture probability P_f is [10]

$$P_f = 1 - \exp\left(-\int_{L_0} \frac{1}{l_0} \left[\frac{\sigma_f(x)}{\sigma_0}\right]^m dx\right) \tag{2}$$

in which σ_0 denotes the fibers strength at the tested gauge length l_0 ; m denotes the fiber Weibull modulus; and L_0 denotes the integral length.

2.1 Life Prediction Model at Room Temperature

The global load sharing (GLS) assumption is used to determine the load carried by intact and fracture fibers.

$$\frac{\sigma}{V_f} = (1 - P_f)T + \langle T_b \rangle P_f \tag{3}$$

in which σ denotes the applied stress; V_f denotes the fiber volume fraction; T denotes the stress carried by intact fibers; and $\langle T_b \rangle$ denotes the average stress carried by broken fibers.

$$\langle T_b \rangle = \frac{T}{P_f} \left(\frac{\sigma_c}{T}\right)^{m+1} \left(\frac{\sigma_o(N)}{\sigma_o}\right)^m \frac{\tau_i(N)}{\tau_i} \left\{ 1 - \exp\left[-\left(\frac{T}{\sigma_c}\right)^{m+1} \left(\frac{\sigma_o}{\sigma_o(N)}\right)^m \frac{\tau_i}{\tau_i(N)}\right] \right\} - \frac{T}{P_f} \exp\left\{-\left(\frac{T}{\sigma_c}\right)^{m+1} \left(\frac{\sigma_o}{\sigma_o(N)}\right)^m \frac{\tau_i}{\tau_i(N)}\right\} \tag{4}$$

and

$$P_f = 1 - \exp\left\{-\left(\frac{T}{\sigma_c}\right)^{m+1} \left(\frac{\sigma_o}{\sigma_o(N)}\right)^m \frac{\tau_i}{\tau_i(N)}\right\} \tag{5}$$

The interface shear stress at different cycle number $\tau_i(N)$ is determined by Eq. (6). [11]

$$\tau_i(N) = \tau_{i0} + [1 - \exp(-\omega N^\lambda)](\tau_{imin} - \tau_{i0}) \tag{6}$$

in which τ_{i0} denotes the initial interface shear stress; τ_{imin} denotes the steady-state interface shear stress under cyclic loading; and ω and λ are empirical constants.

The variation in fibers strength $\sigma_o(N)$ is given by Eq. (7). [12]

$$\sigma_o(N) = \sigma_o [1 - p_1 (\log N)^{p_2}] \tag{7}$$

where p_1 and p_2 are empirical parameters.

Substituting Eqs. (4) and (5) into Eq. (3), it leads to the form of

$$\frac{\sigma}{V_f} = T \left(\frac{\sigma_c}{T}\right)^{m+1} \left(\frac{\sigma_o(N)}{\sigma_o}\right)^m \frac{\tau_i(N)}{\tau_i} \left\{ 1 - \exp \left[- \left(\frac{T}{\sigma_c}\right)^{m+1} \left(\frac{\sigma_o}{\sigma_o(N)}\right)^m \frac{\tau_i}{\tau_i(N)} \right] \right\} \tag{8}$$

Using Eqs. (6), (7) and (8), the stress T carried by intact fibers at the matrix cracking plane can be determined for different fatigue peak stresses. Substituting Eqs. (6), (7) and the intact fibers stress T into Eq. (5), the fibers failure probability corresponding to different cycle number can be determined. When the broken fibers fraction approaches to the critical value q , the composites fatigue fracture.

2.2 Life Prediction Model at Elevated Temperature

When fiber-reinforced CMCs subjected to oxidation, the notch would form at the fibers surface leading to degradation of fibers strength and the increase of fiber stress concentration and fracture probability. The fracture probabilities of oxidized fibers in the oxidation region, unoxidized fibers in the oxidation region, fibers in the interface debonded region and interface bonded region of P_{fa} , P_{fb} , P_{fc} and P_{fd} are

$$P_{fa} = 1 - \exp \left\{ -2 \frac{l_t}{l_0} \left[\frac{T}{\sigma_o(t)} \right]^m \right\} \tag{9a}$$

$$P_{fb} = 1 - \exp \left\{ -2 \frac{l_t}{l_0} \left(\frac{T}{\sigma_o} \right)^m \right\} \tag{9b}$$

$$P_{fc} = 1 - \exp \left\{ - \frac{r_f T^{m+1}}{l_0 (\sigma_o(N))^m \tau_i(N) (m+1)} \left[1 - \left(1 - \frac{l_d(N)}{l_f(N)} \right)^{m+1} \right] \right\} \tag{9c}$$

$$P_{fd} = 1 - \exp \left\{ - \frac{2r_f T^m}{\rho l_0 (\sigma_o(N))^m (m+1) \left(1 - \frac{\sigma_{fo}}{T} \frac{l_d(N)}{l_s(N)} \right)} \times \left[\left(1 - \frac{l_d(N)}{l_f(N)} \right) - \left(1 - \frac{\sigma_{fo}}{T} \frac{l_d(N)}{l_f(N)} \right) \frac{\rho l_c}{2r_f} \right]^{m+1} \right\} \tag{9d}$$

where r_f denotes the fiber radius; l_d denotes the interface debonded length; l_c denotes the matrix crack spacing; ρ denotes the shear-lag model parameter; σ_{fo} denotes the fiber stress at the interface bonded region; and l_f denotes the slip length over which the fiber stress would

decay to zero if not interrupted by the far-field equilibrium stresses; and l_t denotes the oxidation region length. [13]

$$l_t = \varphi_1(1 - e^{-\varphi_2 t}) \tag{10}$$

where φ_1 and φ_2 are fitting parameters dependent on temperature. $\sigma_0(t)$ denotes the time dependence of fibers strength. [14]

$$\sigma_0(t) = \sigma_0, t \leq \frac{1}{k} \left(\frac{K_{IC}}{Y\sigma_0} \right)^4 \tag{11a}$$

$$\sigma_0(t) = \frac{K_{IC}}{Y\sqrt[4]{kt}}, t > \frac{1}{k} \left(\frac{K_{IC}}{Y\sigma_0} \right)^4 \tag{11b}$$

where K_{IC} denotes the critical stress intensity factor; Y is a geometric parameter; and k is the parabolic rate constant.

The GLS assumption is used to determine the load carried by intact and fracture fibers [10].

$$\frac{\sigma}{V_f} = \left[1 - P_f \left(1 + \frac{2l_f}{l_c} \right) \right] T + P_r \frac{2l_f}{l_c} \langle T_b \rangle \tag{12}$$

where

$$P_f = \varphi [\eta P_{fa} + (1 - \eta) P_{fb}] + P_{fc} + P_{fd} \tag{13a}$$

$$P_r = P_{jc} + P_{jd} \tag{13b}$$

where η denotes the oxidation fibers fraction in the oxidized region; and φ denotes the fraction of oxidation in the multiple matrix cracks.

$$\varphi = \frac{l_{sat}}{l_f - 2l_t} \tag{14}$$

where l_{sat} denotes the saturation matrix crack spacing.

The average stress carried by broken fibers is given by Eq. (15).

$$\begin{aligned} \langle T_b \rangle &= \int_0^{l_t} T_b(x) f(x) dx \\ &= \frac{T}{P_r} \left(\frac{\sigma_c}{T} \right)^{m+1} \left(\frac{\sigma_0(N)}{\sigma_0} \right)^m \frac{\tau_i(N)}{\tau_i} \left\{ 1 - \exp \left[- \left(\frac{T}{\sigma_c} \right)^{m+1} \left(\frac{\sigma_0}{\sigma_0(N)} \right)^m \frac{\tau_i}{\tau_i(N)} \right] \right\} \\ &\quad - \frac{T}{P_r} \exp \left\{ - \left(\frac{T}{\sigma_c} \right)^{m+1} \left(\frac{\sigma_0}{\sigma_0(N)} \right)^m \frac{\tau_i}{\tau_i(N)} \right\} \end{aligned} \tag{15}$$

Substituting Eqs. (13) and (15) into Eq. (12), the stress T carried by intact fibers at the matrix cracking plane can be determined for different cycle number and fatigue stress. Substituting Eqs. (6), (7), (10) and (11) and the intact fiber stress T into Eq. (9), the fibers

failure probabilities of oxidized fibers in the oxidation region, unoxidized fibers in the oxidation region, fibers in the interface debonded region and interface bonded region can be determined for different number of applied cycles.

3 Results and Discussion

3.1 Unidirectional C/SiC Composite

The monotonic tensile strength is 270 MPa at room temperature, and the fatigue peak stresses are 0.51, 0.66, 0.74, 0.88 and 0.96 tensile strength; and the monotonic tensile strength is 320 MPa at 800 °C in air, and the fatigue peak stresses are 0.37, 0.43, 0.56, 0.65 and 0.78 tensile strength [15].

The experimental and theoretical fatigue life S–N curves at room temperature and 800 °C in air are illustrated in Fig. 1a. The fatigue limit at room temperature is 0.88 tensile strength, and 0.22 tensile strength at 800 °C in air. The broken fibers fraction versus cycle number curves under 0.88 and 0.96 tensile strength at room temperature are given in Fig. 1b. When $\sigma_{\max}=0.96$ and $0.88 \sigma_{\text{UTS}}$, the composite experienced 93,424 and 1,000,000 cycles, respectively. The broken fibers fraction versus cycle number curves under 0.37, 0.43, 0.56, 0.65 and 0.78 tensile strength at 800 °C in air are given in Fig. 1c. When $\sigma_{\max}=0.78, 0.65, 0.56, 0.43$ and $0.37 \sigma_{\text{UTS}}$, the composite experienced 3133, 9957, 21,245, 48,578 and 102,952 cycles, respectively. The broken fibers fraction versus cycle number curves under 0.9 and $0.95 \sigma_{\text{UTS}}$ at room temperature and 800 °C in air are given in Fig. 1d. When $\sigma_{\max}=0.95 \sigma_{\text{UTS}}$, the composite experienced 277,006 cycles at room temperature, and 30 cycles at 800 °C in air; and when $\sigma_{\max}=0.9 \sigma_{\text{UTS}}$, the composite experienced 1,000,000 cycles at room temperature, and 374 cycles at 800 °C in air.

3.2 Cross-ply C/SiC Composite

The monotonic tensile strength of cross-ply C/SiC composite is 124 MPa at room temperature, and the fatigue peak stresses are 0.70, 0.80, 0.85 and 0.9 tensile strength; and the monotonic tensile strength of cross-ply C/SiC composite is 150 MPa at 800 °C in air, and the fatigue peak stresses are 0.6, 0.65 and 0.7 tensile strength [15].

The experimental and theoretical fatigue life S–N curves at room temperature and 800 °C in air are illustrated in Fig. 2a. The fatigue limit at room temperature is 0.85 tensile strength, and 0.26 tensile strength at 800 °C in air. The broken fibers fraction versus cycle number curves under 0.85 and 0.9 tensile strength at room temperature are given in Fig. 2b. When $\sigma_{\max}=0.9$ and $0.85 \sigma_{\text{UTS}}$, the composite experienced 389,371 and 1,000,000 cycles, respectively. The broken fibers fraction versus cycle number curves under 0.6, 0.65 and 0.7 tensile strength at 800 °C in air are given in Fig. 2c. When $\sigma_{\max}=0.7, 0.65$ and $0.6 \sigma_{\text{UTS}}$, the composite experienced 1474, 2486 and 3643 cycles, respectively. The broken fibers fraction versus cycle number curves under 0.8 tensile strength at room temperature and 800 °C in air are given in Fig. 2d. When $\sigma_{\max}=0.8 \sigma_{\text{UTS}}$, the composite experienced 1,000,000 cycles at room temperature, and 75 cycles at 800 °C in air.

3.3 2D C/SiC Composite

The monotonic tensile strength of 2D C/SiC composite is 420 MPa at room temperature, and the fatigue peak stresses are 0.80, 0.83, 0.86, 0.89, 0.91 and 0.96 tensile strength [16]; and the

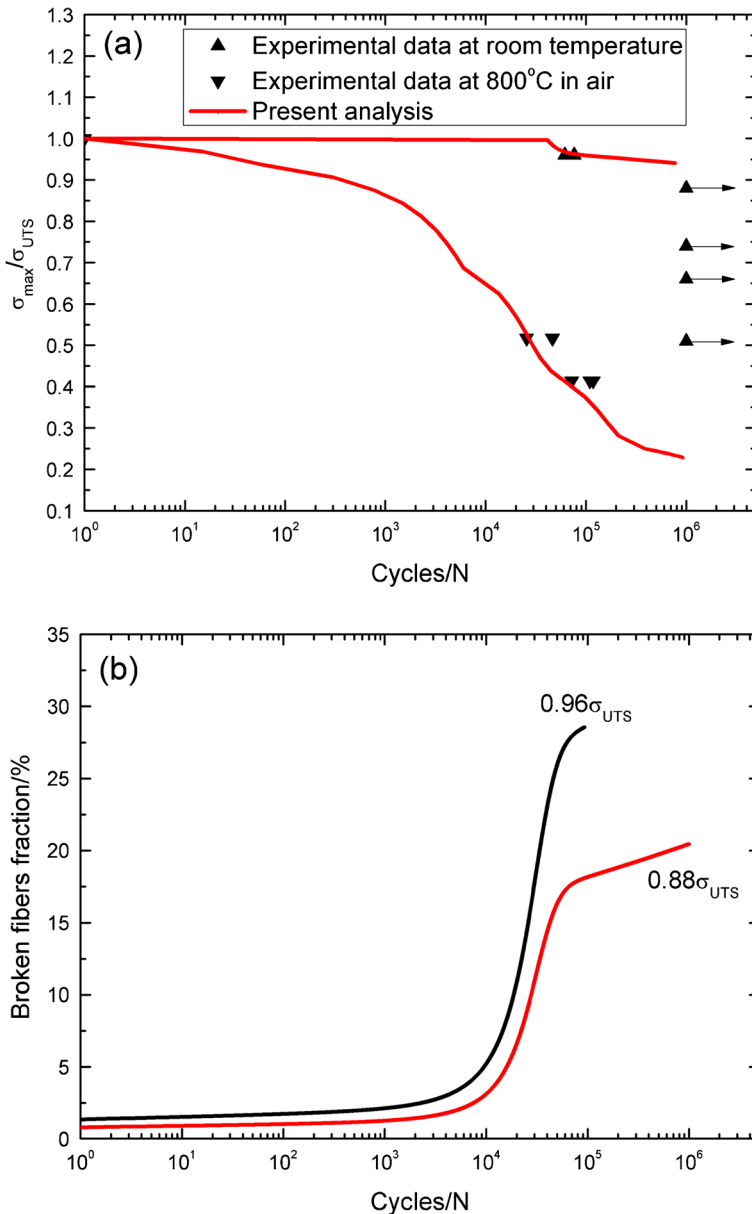


Fig. 1 **a** The fatigue life S–N curves of experimental data and theoretical analysis at room temperature and 800 °C in air; **b** the broken fibers fraction versus cycle number under 0.96 and 0.88 σ_{UTS} at room temperature; **c** the broken fibers fraction versus cycle number under 0.37, 0.43, 0.56, 0.65 and 0.78 σ_{UTS} at 800 °C in air; and **d** the broken fibers fraction versus cycle number under 0.9 and 0.95 σ_{UTS} at room temperature and 800 °C in air of unidirectional C/SiC composite

monotonic tensile strength of 2D C/SiC composite is 487 MPa at 550 °C in air, and the fatigue peak stresses are 0.22, 0.36, 0.56 and 0.72 tensile strength [17].

The experimental and theoretical fatigue life S–N curves at room temperature and 550 °C in air are illustrated in Fig. 3a. The fatigue limit at room temperature is 0.83 tensile strength, and

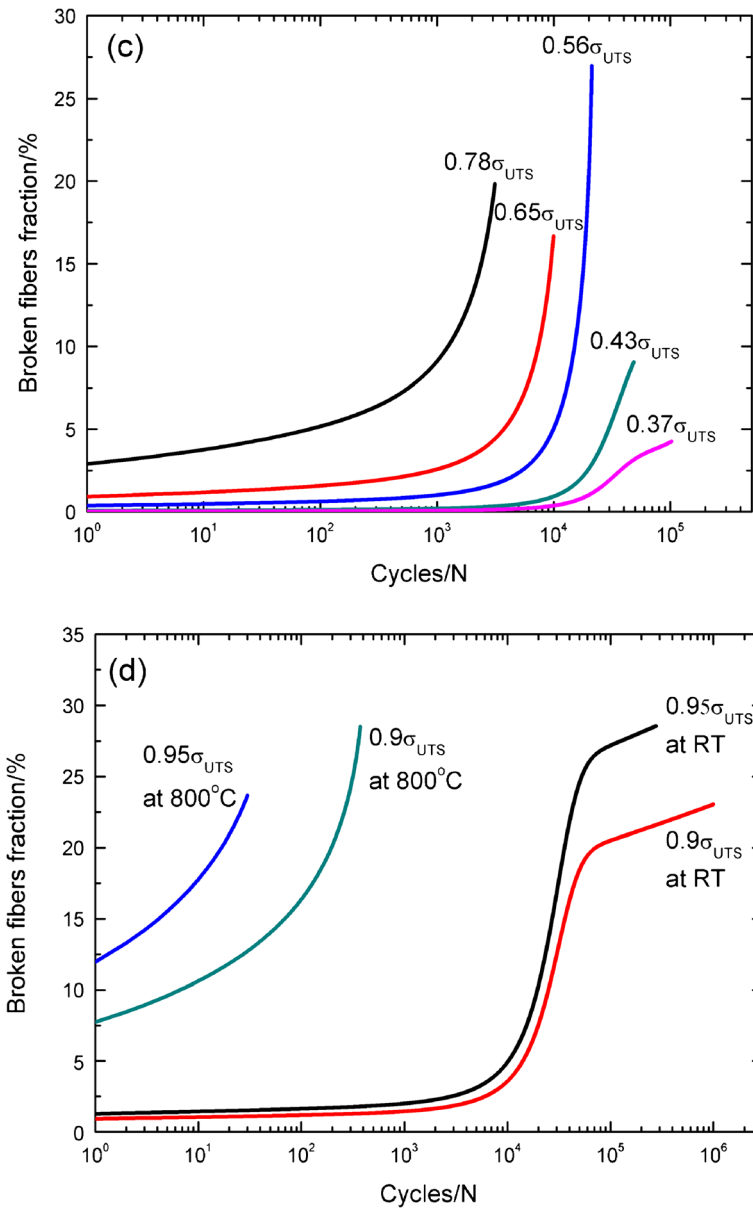


Fig. 1 (continued)

0.3 tensile strength at 550°C in air. The broken fibers fraction versus cycle number curves under 0.8, 0.83, 0.86, 0.89, 0.91 and 0.96 tensile strength at room temperature are given in Fig. 3b. When $\sigma_{\max} = 0.96, 0.91, 0.89, 0.86, 0.83$ and $0.8 \sigma_{UTS}$, the composite experienced 2009, 28,237, 93,029, 550,740, 1,000,000 and 1,000,000 cycles, respectively. The broken fibers fraction versus cycle number curves under 0.22, 0.36, 0.56 and 0.72 tensile strength at 550°C in air are given in Fig. 3c. When $\sigma_{\max} = 0.72, 0.56, 0.36$ and $0.22 \sigma_{UTS}$, the composite

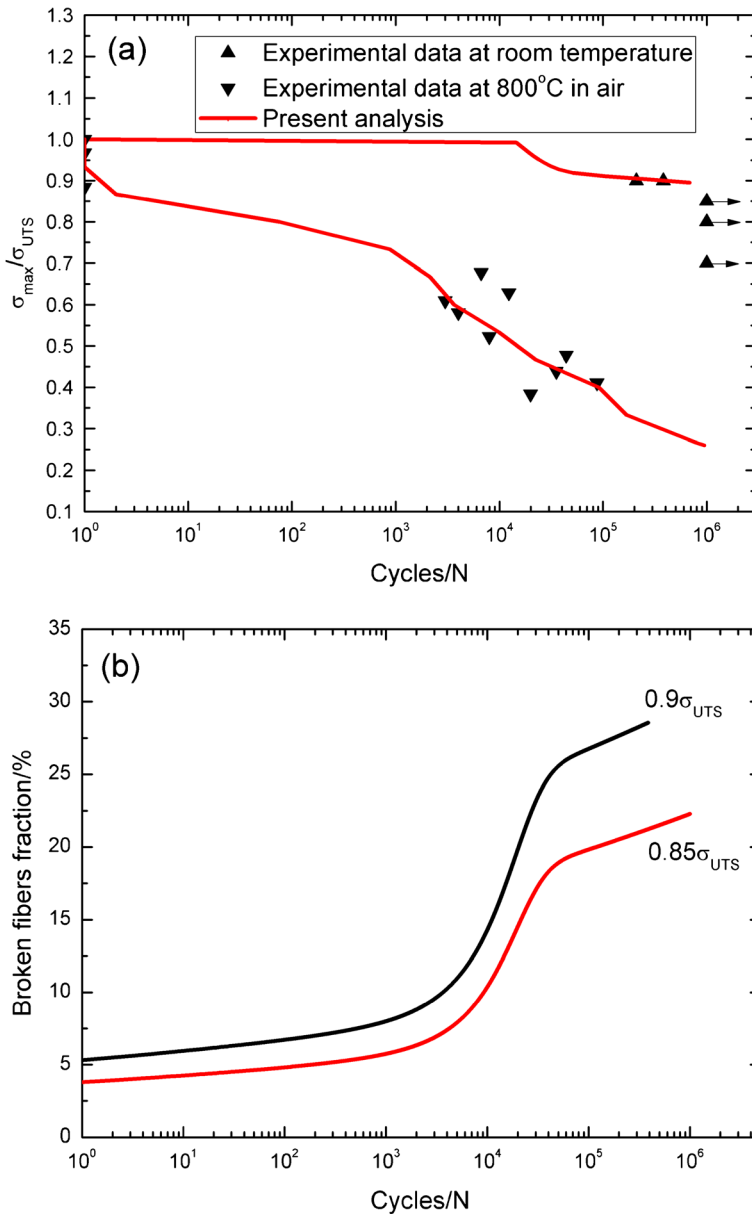


Fig. 2 **a** The fatigue life S–N curves of experimental data and theoretical analysis at room temperature and 800 °C in air; **b** the broken fibers fraction versus cycle number under 0.9 and 0.85 σ_{UTS} at room temperature; **c** the broken fibers fraction versus cycle number under 0.6, 0.65 and 0.7 σ_{UTS} at 800 °C in air; and **d** the broken fibers fraction versus cycle number under 0.8 σ_{UTS} at room temperature and 800 °C in air of cross-ply C/SiC composite

experienced 3514, 24,840, 183,651 and 1,000,000 cycles, respectively. The broken fibers fraction versus cycle number curves under 0.85 tensile strength at room temperature and 550 °C in air are given in Fig. 3d. When $\sigma_{max}=0.85\sigma_{UTS}$, the composite experienced 1,000,000 cycles at room temperature, and 42 cycles at 550 °C in air.

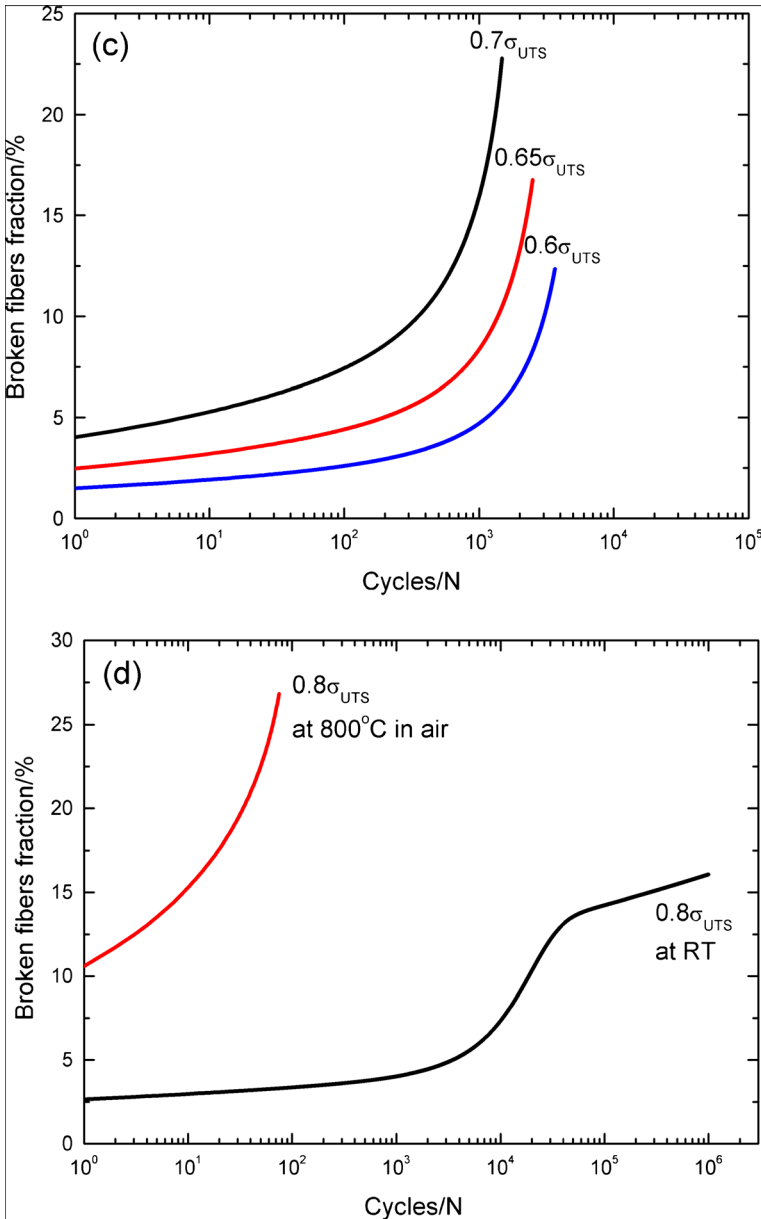


Fig. 2 (continued)

3.4 2.5D C/SiC Composite

The monotonic tensile strength of 2.5D C/SiC composite is 212 MPa at room temperature, and the fatigue peak stresses are 0.85, 0.89, 0.94, 0.96 and 0.99 tensile

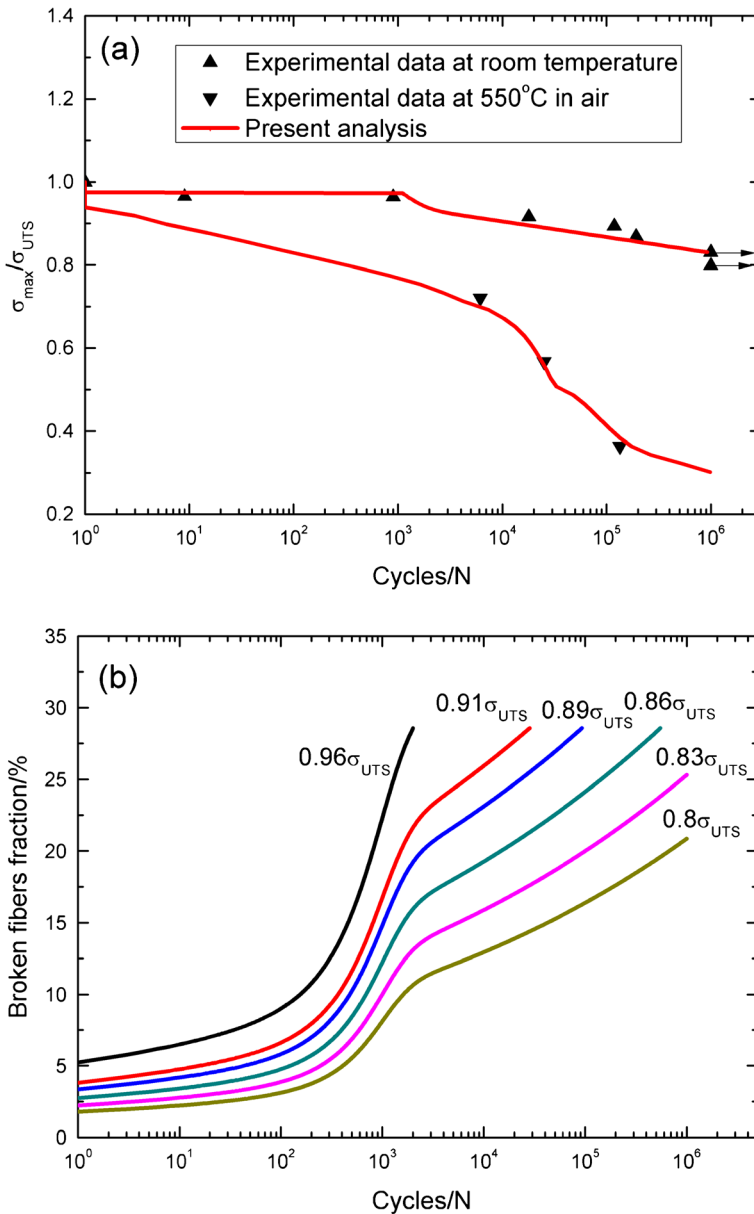


Fig. 3 **a** The fatigue life S–N curves of experimental data and theoretical analysis at room temperature and 550 °C in air; **b** the broken fibers fraction versus cycle number under 0.8, 0.83, 0.86, 0.89, 0.91 and 0.96 σ_{UTS} at room temperature; **c** the broken fibers fraction versus cycle number under 0.22, 0.36, 0.56 and 0.72 σ_{UTS} at 550 °C in air; and **d** the broken fibers fraction versus cycle number under 0.85 σ_{UTS} at room temperature and 550 °C in air of 2D C/SiC composite

strength [18]; and the monotonic tensile strength of 2.5D C/SiC composite is 280 MPa at 800 °C in air, and the fatigue peak stresses are 0.5, 0.6, 0.7 and 0.8 tensile strength [19].

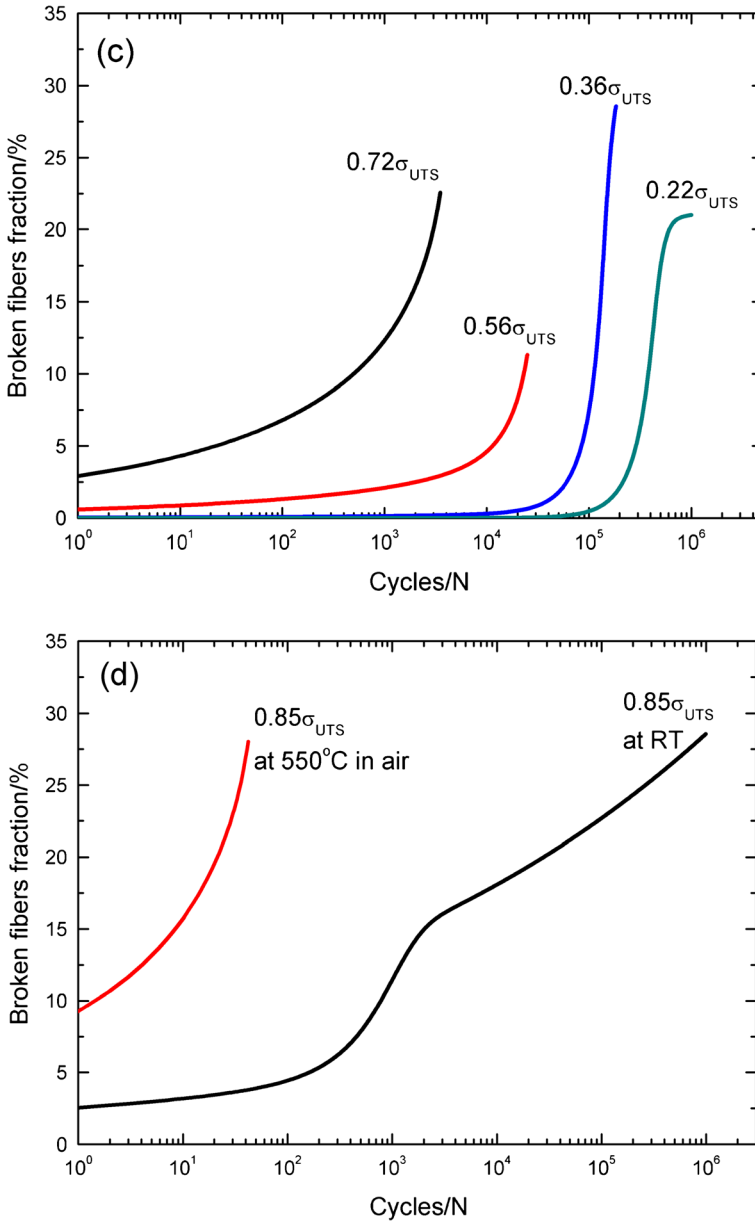


Fig. 3 (continued)

The experimental and theoretical fatigue life S–N curves at room temperature and 800°C in air are illustrated in Fig. 4a. The fatigue limit at room temperature is 0.85 tensile strength, and 0.28 tensile strength at 800°C in air. The broken fibers fraction versus cycle number curves under 0.85 , 0.89 , 0.94 , 0.96 and 0.99 tensile strength at

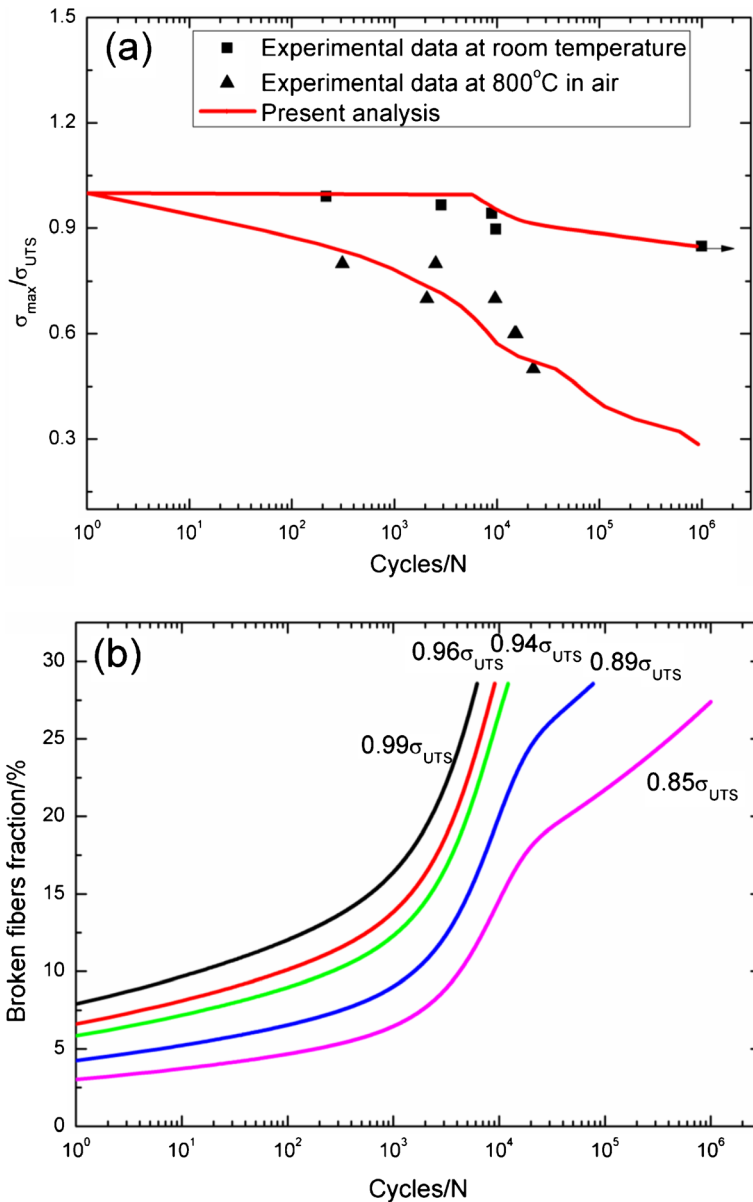


Fig. 4 a The fatigue life S–N curves of experimental data and theoretical analysis at room temperature and 800 °C in air; b the broken fibers fraction versus cycle number under 0.85, 0.89, 0.94, 0.96 and 0.99 σ_{UTS} at room temperature; c the broken fibers fraction versus cycle number under 0.5, 0.6, 0.7 and 0.8 σ_{UTS} at 800 °C in air; and d the broken fibers fraction versus cycle number under 0.8 σ_{UTS} at room temperature and 800 °C in air of 2.5D C/SiC composite

room temperature are given in Fig. 4b. When $\sigma_{max}=0.99, 0.96, 0.94, 0.89$ and $0.85 \sigma_{UTS}$, the composite experienced 6182, 9084, 12,173, 77,354 and 1,000,000 cycles,

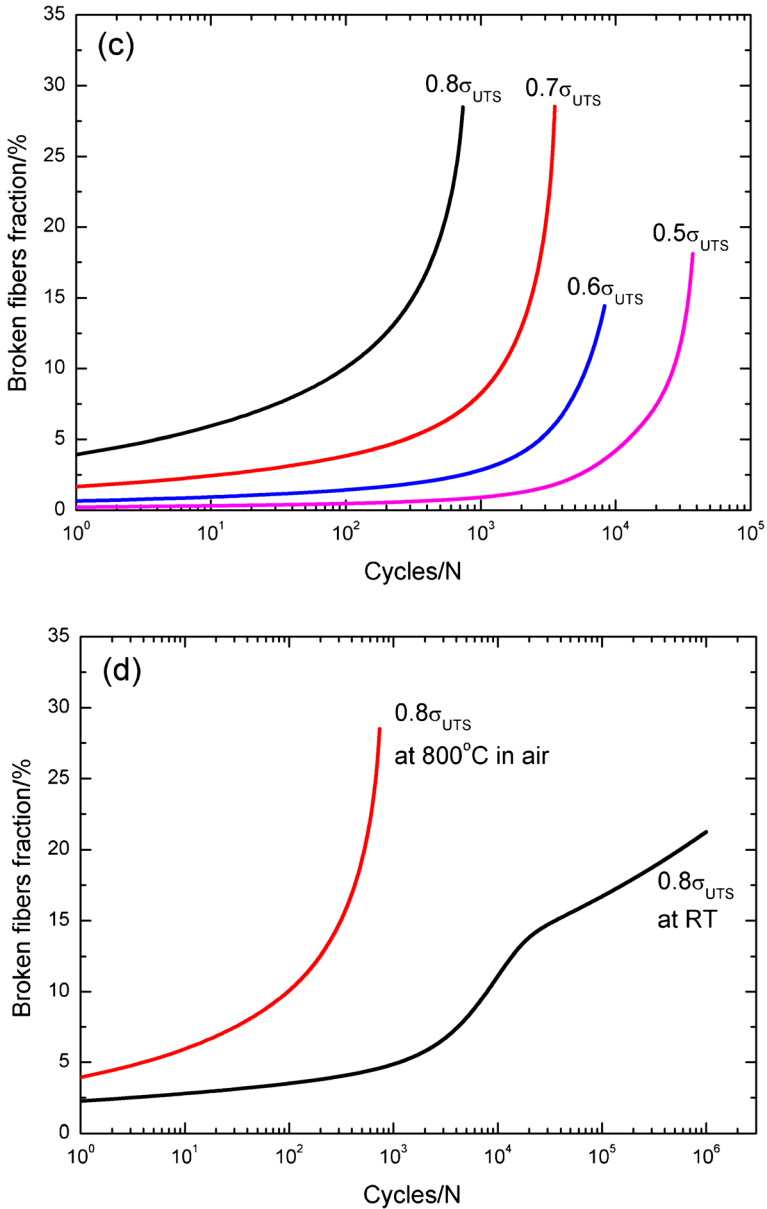


Fig. 4 (continued)

respectively. The broken fibers fraction versus cycle number curves under 0.5, 0.6, 0.7 and 0.8 tensile strength at 800°C in air are given in Fig. 4c. When $\sigma_{\max}=0.8, 0.7, 0.6$ and $0.5 \sigma_{UTS}$, the composite experienced 736, 3525, 8314 and 37,308 cycles, respectively. The broken fibers fraction versus cycle number curves under 0.8 tensile strength at room temperature and 800°C in air are given in Fig. 4d. When $\sigma_{\max}=0.8$

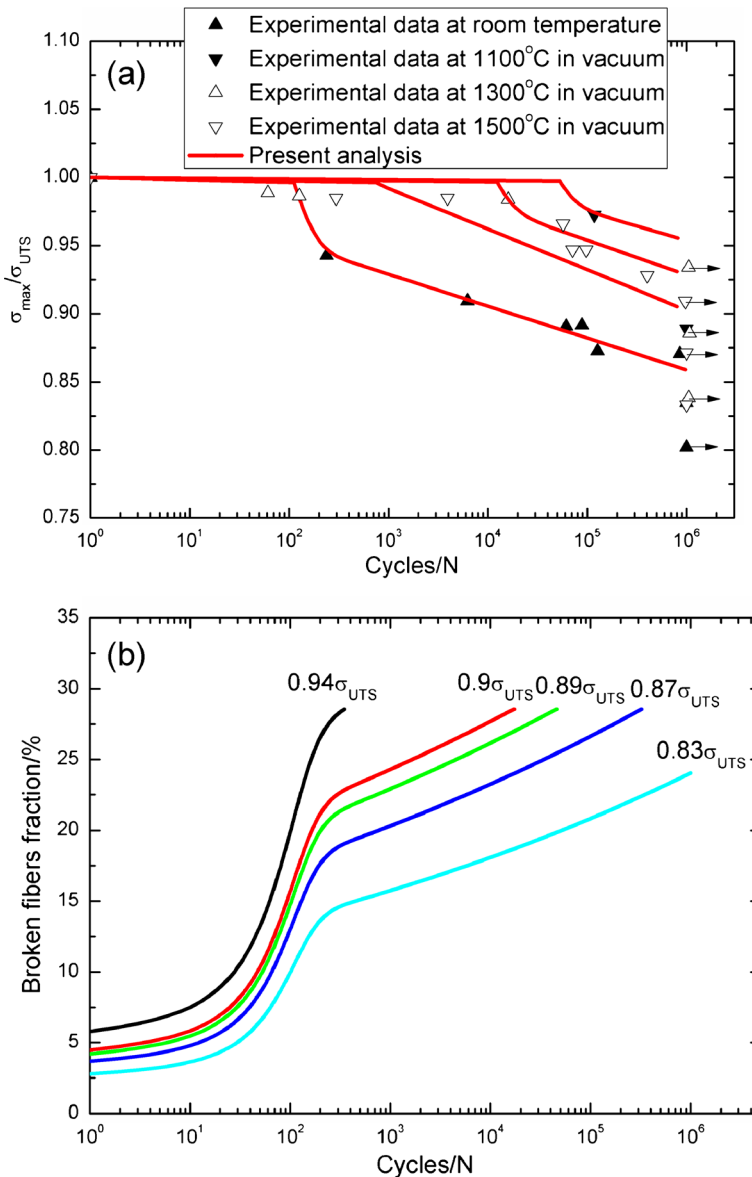


Fig. 5 **a** The fatigue life S–N curves of experimental data and theoretical analysis at room temperature, 1100, 1300 and 1500 °C in vacuum; **b** the broken fibers fraction versus cycle number under 0.83, 0.87, 0.89, 0.9 and 0.94 σ_{UTS} at room temperature; **c** the broken fibers fraction versus cycle number under 0.88 and 0.97 σ_{UTS} at 1100 °C in vacuum; **d** the broken fibers fraction versus cycle number under 0.83, 0.93, 0.98 and 0.99 σ_{UTS} at 1300 °C in vacuum; **e** the broken fibers fraction versus cycle number under 0.9, 0.92, 0.95, 0.96 and 0.98 σ_{UTS} at 1500 °C in vacuum; and **f** the broken fibers fraction versus cycle number under 0.95 σ_{UTS} at room temperature, 1100, 1300 and 1500 °C in vacuum of 3D C/SiC composite

σ_{UTS} , the composite experienced 1,000,000 cycles at room temperature, and 736 cycles at 800 °C in air.

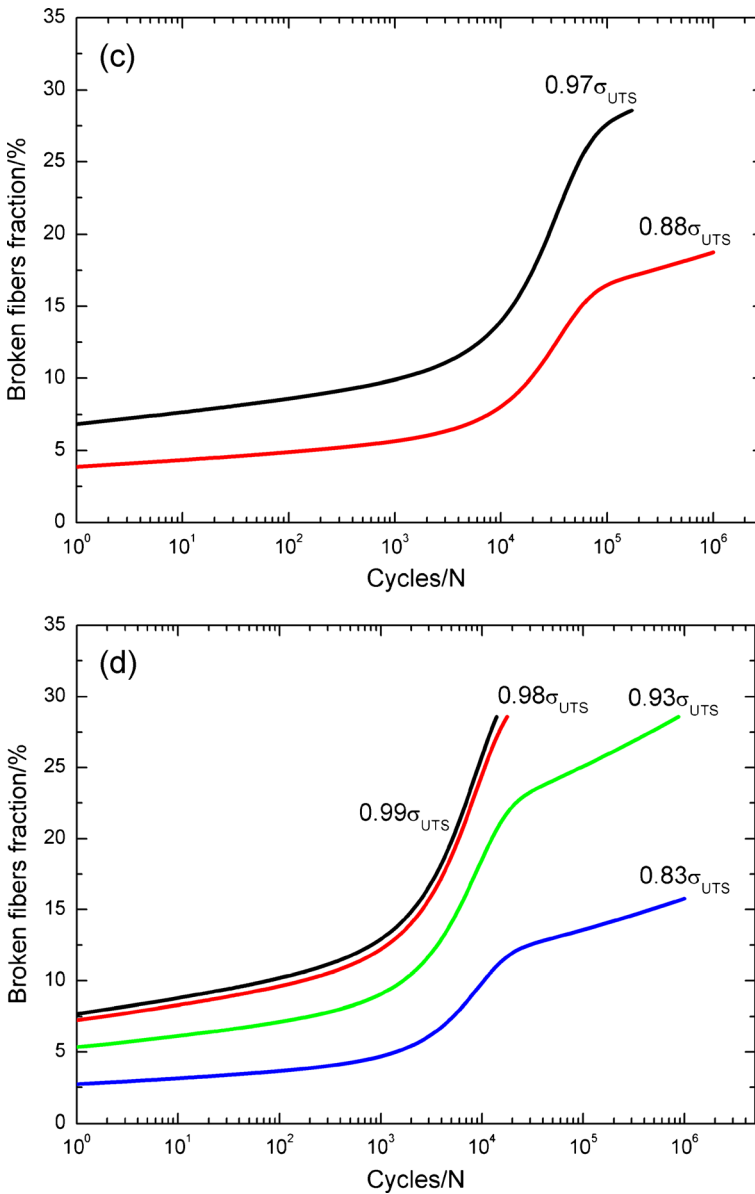


Fig. 5 (continued)

3.5 3D C/SiC Composite

The monotonic tensile strength is 276 MPa at room temperature, and the fatigue peak stress are 0.80, 0.83, 0.87, 0.89, 0.90 and 0.94 tensile strength [20]; the monotonic tensile strength is 360 MPa at 1100 °C in 10^{-4} Pa vacuum, and the fatigue peak stresses are 0.97 and 0.88 tensile strength [21]; the monotonic tensile strength is

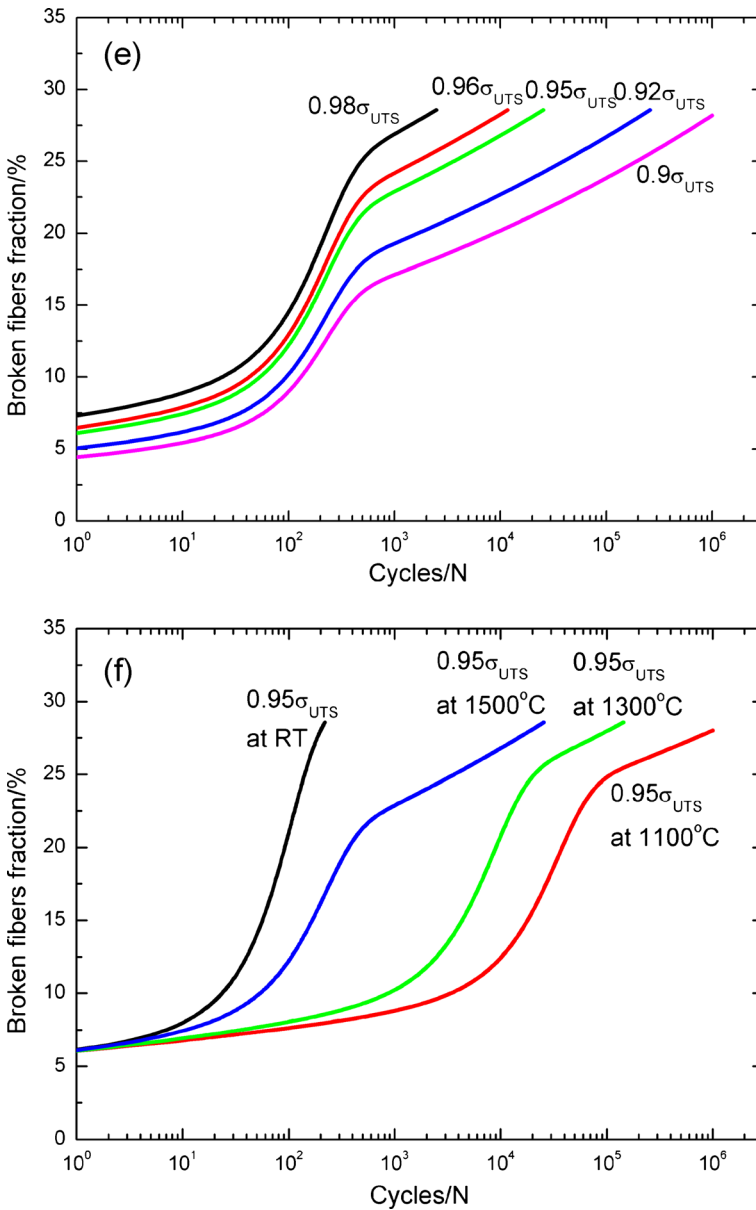


Fig. 5 (continued)

304 MPa at 1300 °C in 10^{-4} Pa vacuum, and the fatigue peak stresses are 0.5, 0.83, 0.93, 0.98 and 0.99 tensile strength [20]; and the monotonic tensile strength is 261 MPa at 1500 °C in 10^{-4} Pa vacuum, and the fatigue peak stresses are 0.98, 0.96, 0.95, 0.92, 0.9, 0.87 and 0.83 tensile strength [22].

The experimental and theoretical fatigue life S–N curves at room temperature, 1100, 1300 and 1500 °C in vacuum are illustrated in Fig. 5a. The fatigue limit at room temperature is 0.86

tensile strength, 0.95 tensile strength at 1100 °C in 10^{-4} Pa vacuum, 0.93 tensile strength at 1300 °C in 10^{-4} Pa vacuum, and 0.9 tensile strength at 1500 °C in 10^{-4} Pa vacuum. The broken fibers fraction versus cycle number curves under 0.94, 0.9, 0.89, 0.87 and 0.83 σ_{UTS} at room temperature are given in Fig. 5b. When $\sigma_{max}=0.94, 0.9, 0.89, 0.87$ and $0.83 \sigma_{UTS}$, the composite experienced 349, 17,233, 45,914, 323,787 and 1,000,000 cycles, respectively. The broken fibers fraction versus cycle number curves under 0.88 and 0.97 tensile strength at 1100 °C in 10^{-4} Pa vacuum are given in Fig. 5c. When $\sigma_{max}=0.97$ and $0.88 \sigma_{UTS}$, the composite experienced 171,281 and 1,000,000 cycles, respectively. The broken fibers fraction versus cycle number curves under 0.99, 0.98, 0.93 and 0.83 tensile strength at 1300 °C in 10^{-4} Pa vacuum are given in Fig. 5d. When $\sigma_{max}=0.99, 0.98, 0.93$ and $0.83 \sigma_{UTS}$, the composite experienced 14,008, 17,740, 870,731 and 1,000,000 cycles, respectively. The broken fibers fraction versus cycle number curves under 0.98, 0.96, 0.95, 0.92 and 0.9 tensile strength at 1500 °C in 10^{-4} Pa vacuum are given in Fig. 5e. When $\sigma_{max}=0.98, 0.96, 0.95, 0.92$ and $0.9 \sigma_{UTS}$, the composite experienced 2493, 11,799, 25,608, 259,213 and 1,000,000 cycles, respectively. The broken fibers fraction versus cycle number curves under 0.95 tensile strength at room temperature, 1100, 1300 and 1500 °C in 10^{-4} Pa vacuum are given in Fig. 5f. When $\sigma_{max}=0.95 \sigma_{UTS}$, the composite experienced 219 cycles a at room temperature, 1,000,000 cycles at 1100 °C, 143,725 cycles at 1300 °C, and 25,608 cycles at 1500 °C in 10^{-4} Pa vacuum.

3.6 Discussion

At room temperature, the fatigue limit corresponding to unidirectional, cross-ply, 2D, 2.5D and 3D C/SiC composites are 0.88, 0.85, 0.83, 0.85 and 0.86 tensile strength. The total fiber volume fraction of unidirectional, cross-ply, 2D, 2.5D and 3D C/SiC composites are 40, 40, 45, 40 and 40 %, respectively. The ECFL for unidirectional, cross-ply, 2D, 2.5D and 3D C/SiC are 40, 20, 22.5, 30 and 37 %. For unidirectional and 3D C/SiC composites with high ECFL, i.e., 40 and 37 %, the fatigue limits are 0.88 and 0.86 tensile strength, respectively. For cross-ply, 2D and 2.5D C/SiC composites, the fatigue limit of cross-ply C/SiC composite is 0.85 tensile strength with ECFL of 20 %; the fatigue limit of 2.5D C/SiC composite is also 0.85 tensile strength, however with higher ECFL of 30 % due to fibers bending inside of the composite; and the fatigue limit of 2D C/SiC composite is 0.83 tensile strength with ECFL of 20 % also due to fibers bending in the preform.

At 550 °C in air, the fatigue limit of 2D C/SiC composite is 0.3 tensile strength; and at 800 °C in air condition, the fatigue limits of unidirectional, cross-ply, and 2.5D C/SiC composites are 0.22, 0.26 and 0.28 tensile strength. With increasing oxidation temperature, the fatigue limit of C/SiC composite decreases. And at the same oxidation temperature, the fatigue limit of unidirectional C/SiC composite decreases the most rapidly, i.e., from 0.88 tensile strength at room temperature to 0.22 tensile strength at 800 °C in air, with the highest fiber volume fraction along the loading direction; the fatigue limit of 2.5D C/SiC composite is the highest among the three C/SiC composites at 800 °C in air, due to high ECFL and the protection of transverse yarns from the outside environment; and the fatigue limit of cross-ply C/SiC

composite lies in the middle, i.e., between unidirectional and 2.5D C/SiC composite, due to low ECFL compared with 2.5D C/SiC composite, and the protection of transverse plies from the outside environment compared with unidirectional C/SiC composite.

For 3D C/SiC composite, the fatigue limits at 1100, 1300 and 1500 °C in 10^{-4} Pa vacuum are 0.95, 0.93 and 0.9 tensile strength, which are all higher than the fatigue limit at room temperature, i.e., 0.86 tensile strength. As the radial thermal residual tensile stress existed in the fiber/matrix interface due to the large mismatch of the radial thermal expansion coefficient between carbon fibers and silicon carbide matrix, i.e., $7 \times 10^{-6}/^{\circ}\text{C}$ vs $4.8 \times 10^{-6}/^{\circ}\text{C}$, when the composite was cooled down from the high fabricated temperature, i.e., 950 to 1000 °C, the interface shear stress is low, and decreases rapidly at room temperature; at 1100, 1300 and 1500 °C, the interface shear stress increases and decreases slowly, due to radial thermal residual compressive stress; however, at 1300 and 1500 °C, the interface shear stress is such high that matrix cracks propagate through the fiber/matrix interface, leading to the decrease of fatigue limit compared with that at 1100 °C.

4 Conclusions

The effects of temperature, oxidation and fiber preforms on the fatigue life of C/SiC composites have been analyzed. An effective coefficient of the fiber volume fraction along the loading direction (ECFL) was introduced to describe the fiber architecture of the preforms. The broken fibers fraction under cyclic fatigue loading considering the degradation of interface shear stress and fibers strength was obtained. The fatigue life S–N curves and fatigue limits of unidirectional, cross-ply, 2D, 2.5D and 3D C/SiC composites have been predicted.

- (1) At room temperature, the fatigue limits of unidirectional, cross-ply, 2D, 2.5D and 3D C/SiC composites are 0.88, 0.85, 0.83, 0.85 and 0.86 tensile strength. The unidirectional and 3D C/SiC composites with high ECFL have the high fatigue limit compared with that of cross-ply, 2D and 2.5D C/SiC composites.
- (2) At 550 °C in air, the fatigue limit of 2D C/SiC composite is 0.3 tensile strength; and at 800 °C in air, the fatigue limits of unidirectional, cross-ply, and 2.5D C/SiC composites are 0.22, 0.26 and 0.28 tensile strength. The fatigue limit decreases with increasing oxidation temperature.
- (3) For 3D C/SiC composite, the fatigue limits at 1100, 1300 and 1500 °C in 10^{-4} Pa vacuum are 0.95, 0.93 and 0.9 tensile strength, which are all higher than the fatigue limit at room temperature, i.e., 0.86 tensile strength, due to radial thermal compressive stress at elevated temperatures.
- (4) Compared with S–N curves at room temperature or at elevated temperature in vacuum environments, the fatigue life S–N curves at elevated temperature in oxidized atmosphere exhibit an apparent region, in which the fatigue life decreases rapidly due to oxidation.

Acknowledgments The author thanks the Science and Technology Department of Jiangsu Province for the funding that made this research study possible

Compliance with Ethical Standards

Funding This study has received the support from the Science and Technology Department of Jiangsu Province through the Natural Science Foundation of Jiangsu Province (Grant No. BK20140813), and the Fundamental Research Funds for the Central Universities (Grant No. NS2016070).

Conflict of Interest The author declares that he has no conflict of interest.

References

1. Naslain, R.: Design, preparation and properties of non-oxide CMCs for application in engines and nuclear reactors: an overview. *Compos Sci Technol* **64**, 155–170 (2004). doi:10.1016/S0266-3538(03)00230-6
2. Schmidt, S., Beyer, S., Knabe, H., Immich, H., Meistring, R., Gessler, A.: Advanced ceramic matrix composite materials for current and future propulsion system applications. *Acta Astronaut* **55**, 409–420 (2004). doi:10.1016/j.actaastro.2004.05.052
3. DiCarlo, J.A., Van Roode, M.: Ceramic composite development for gas turbine hot section components. *Proc ASME Turbo Expo Power Land Sea Air* **2**, 221–231 (2006)
4. Stephen, T.: General Electric primes CMC for turbine blades. *Flight International*, 2010. <http://www.flightglobal.com/news/articles/general-electric-primes-cmc-for-turbine-blades-349834/>
5. Gowayed, Y., Ojard, G., Santhosh, U., Jefferso, G.: Modeling of crack density in ceramic matrix composites. *J Compos Mater* **49**, 2285–2294 (2015). doi:10.1177/0021998314545188
6. Li, L.B.: Fatigue hysteresis of carbon fiber-reinforced ceramic-matrix composites at room and elevated temperatures. *Appl Compos Mater* **23**, 1–27 (2016). doi:10.1007/s10443-015-9448-1
7. Li, L.B.: Modeling fatigue hysteresis behavior of unidirectional C/SiC ceramic-matrix composite. *Compos Part B* **66**, 466–474 (2014). doi:10.1016/j.compositesb.2014.06.014
8. Li, L.B.: Fatigue life prediction of carbon fiber-reinforced ceramic-matrix composites at room and elevated temperatures. Part I: Experimental analysis. *Appl Compos Mater* **23**, 101–117 (2016). doi:10.1007/s10443-015-9446-3
9. Li, L.B.: Fatigue life prediction of carbon fiber-reinforced ceramic-matrix composites at room and elevated temperatures. Part II: Experimental comparisons. *Appl Compos Mater* **22**, 961–972 (2015). doi:10.1007/s10443-015-9445-4
10. Curtin, W.A., Ahn, B.K., Takeda, N.: Modeling brittle and tough stress–strain behavior in unidirectional ceramic matrix composites. *Acta Mater* **46**, 3409–3420 (1998). doi:10.1016/S1359-6454(98)00041-X
11. Evans, A.G., Zok, F.W., McMeeking, R.M.: Fatigue of ceramic matrix composites. *Acta Metall Mater* **43**, 859–875 (1995). doi:10.1016/0956-7151(94)00304-Z
12. Lee, S.S., Stinchcomb, W.W.: Damage mechanisms of cross-ply Nicalon/CAS-II laminate under cyclic tension. *Ceram Eng Sci Proc* **15**, 40–48 (1994). doi:10.1002/9780470314500.ch5
13. Lara-Curzio, E.: Analysis of oxidation-assisted stress-rupture of continuous fiber-reinforced ceramic matrix composites at intermediate temperatures. *Compos Part A* **30**, 549–554 (1999). doi:10.1016/S1359-835X(98)00148-1
14. Casas, L., Martinez-Esnaola, J.M.: Modelling the effect of oxidation on the creep behavior of fiber-reinforced ceramic matrix composites. *Acta Mater* **51**, 3745–3757 (2003). doi:10.1016/S1359-6454(03)00189-7
15. Li, L.B.: Fatigue damage models and life prediction of long-fiber-reinforced ceramic matrix composites. PhD Thesis, Nanjing University of Aeronautics and Astronautics, Nanjing, China, 2010.
16. Shuler, S.F., Holmes, J.W., Wu, X.: Influence of loading frequency on the room-temperature fatigue of a carbon-fiber/SiC-matrix composite. *J Am Ceram Soc* **76**, 2327–2336 (1993). doi:10.1111/j.1151-2916.1993.tb07772.x
17. Mall, S., Engesser, J.M.: Effects of frequency on fatigue behavior of CVI C/SiC at elevated temperature. *Compos Sci Technol* **66**, 863–874 (2006). doi:10.1016/j.compscitech.2005.06.020

18. Zhang, C.Y., Wang, X.W., Liu, Y.S., Wang, B., Han, D.: Tensile fatigue of a 2.5D-C/SiC composite at room temperature and 900°C. *Mater. Design* **49**, 814–819 (2013). doi:10.1016/j.matdes.2013.01.076
19. Yang, F.S.: Research on fatigue behavior of 2.5d woven ceramic matrix composites. Master Thesis, Nanjing: Nanjing University of Aeronautics and Astronautics, 2011.
20. Du, S.M., Qiao, S.R., Ji, G.C., Han, D.: Tension-tension fatigue behavior of 3D-C/SiC composite at room temperature and 1300°C. *J Mater Eng* **9**, 22–25 (2002)
21. Liu, X.F.: Tension-tension fatigue behavior of 3D-C/SiC composite at elevated temperature. Master Thesis, Northwestern Polytechnic University 2003.
22. Du, S.M., Qiao, S.R.: Tension-tension fatigue behavior of 3D-C/SiC composite at 1500°C. *J Mater Eng* **5**, 34–36 (2011)